

Pellet Injection as a Possible Tool for Plasma Performance Improvement

A.R. Polevoi 1), M. Sugihara 1), H. Takenaga 2), A. Isayama 2), N. Oyama 2), A. Loarte 3), G. Saibene 3), G.V. Pereverzev 4)

1) ITER International Team ITER Naka Joint Work Site, Mukouyama, Naka-machi, Naka-gun, Ibaraki-ken 311-0193, Japan

2) Japan Atomic Energy Research Institute, Naka Establishment, Japan

3) EFDA, Max-Planck-Institute fur Plasmaphysik, Garching, Germany

4) Max-Planck-Institute fur Plasmaphysik, EUROATOM Association, Garching, Germany

e-mail: polevoa@itergps.naka.jaeri.go.jp

Abstract. ITER operational scenarios with the high field side pellet fuelling are considered. The possibility of reducing the energy losses per edge localised mode (ELM) to an acceptable level is discussed. Requirements on the pellet fuelling system for desirable ELM energy reduction are obtained. Self-consistent transport simulations of pellet fuelled scenarios reveal the possibility of the operation with moderate ELM losses, plasma density below Greenwald density, high energy multiplication factor $Q \sim 20$ and power across the separatrix above the L-H mode power threshold.

1. Introduction

It is clear that peaked density profiles provide higher fusion output in the hot core of the ITER plasma than flat profiles with the same average density and especially with the same pedestal density. High field side (HFS) pellet injection is foreseen in ITER to provide the peaked density profiles. The high-Q operation with pellet fuelling should be compatible with the Greenwald density and the divertor power load limits. This requires special analysis of the pellet fuelled scenarios. Besides fusion gain improvement, pellet injection could provide controllable mitigation of the energy loss due to the type-I edge localised modes (ELMs). As it follows from reference [1], operation with moderate plate loads below a limit:

$$P_{\text{ELM,lim}} \approx 1.05 \text{ MJ/m}^2, \quad (1)$$

helps to achieve a long lifetime of the ITER divertor target. For energy densities higher than $P_{\text{ELM,lim}}$, the number of tolerable ELMs drops substantially. Analysis of the energy loss due to the type-I ELMs relative to the pedestal energy ($\Delta W_{\text{ELM}}/W_p$) [2,3], demonstrates strong reduction of $\Delta W_{\text{ELM}}/W_p$ with increase of the pedestal collisionality v_p^* . Analysis of the JT-60U experiments reveals small ELM fraction $\Delta W_{\text{ELM}}/W_p < 0.10$ and rather weak dependence on collisionality in the range $v_p^* \sim 0.03-0.3$ [4]. But to provide the ITER design robustness we consider here the most pessimistic cases of high ELM energy losses with low collisionality. There are two similar scalings obtained on the basis of the experimental data [2,3]: $\Delta W_{\text{ELM}}/W_p = L_{1,2}$, where $L_1 = (\Delta W_{\text{ELM}}/W_p)_0 / (1 + \tau_{\parallel} / \tau_{\text{ELM}})$, $L_2 = (\Delta W_{\text{ELM}}/W_p)_0 (1 - \exp(-\tau_{\text{ELM}} / \tau_{\parallel}))$, $(\Delta W_{\text{ELM}}/W_p)_0 \approx 0.2$, $\tau_{\text{ELM}} \approx 2.4 \cdot 10^{-4}$ s, $\tau_{\parallel} = 2\pi R q_{95} (1 + (3/2)^{1/2} v_p^*) / c_{s,p}$, $v_p^* = 8.69 \times 10^{-3} \pi R q_{95} n_p / T_p$, R is major plasma radius in [m], q_{95} is a safety factor at 95% of poloidal flux surface, n_p is plasma density at the top of pedestal in [10^{20} m^{-3}], $c_{s,p} = 3 \times 10^5 ((T_{e,p} + T_{i,p}) / M_i)^{1/2}$ is a sound speed evaluated by pedestal temperature in [m/s], $T_p = T_{e,p}$ and $T_{i,p}$ are electron and ion temperatures at the top of pedestal in [keV] and M_i is an ion mass in atomic units. If we use the simplest power dependence as a fitting function for $\Delta W_{\text{ELM}}/W_p$ experimental data [5], we obtain:

$$\Delta W_{\text{ELM}}/W_p = L_3 = 0.064 v_p^{*-0.33}. \quad (2)$$

These v_p^* -dependent experimental scalings of $\Delta W_{\text{ELM}}/W_p$ predict for the ITER reference inductive scenario with spontaneous ELMs a value of $\Delta W_{\text{ELM}}/W_p \sim 10-20\%$, which may exceed $P_{\text{ELM,lim}}$ and substantially reduce the life time of the divertor plates [5]. The general effect of the energy reduction in ELMs with HFS pellet injection has already been obtained in experiments [6,7]. It was found [7] that every pellet produces an ELM, and energy loss during pellet induced ELM obeys the same scaling as spontaneous ELM frequency (f) [8], obtained in JET and ASDEX-U experiments:

$$\Delta W_{\text{ELM}}/W_{\text{tot}} = 0.2 (f\tau_E)^{-1}, \quad f \Delta W_{\text{ELM}} = 0.2 P_{\text{loss}} W_{\text{tot}}/W_{\text{th}}, \quad (3)$$

where $W_{\text{tot}}/W_{\text{th}} \sim 1$ is a ratio of total and thermal energy content, τ_E is the plasma energy confinement time, $P_{\text{loss}} = W_{\text{th}}/\tau_E$ is a power loss to the divertor in the stationary state. On the other hand, it is clear that pellet ablation and mass relocation to the pedestal area increases the pedestal collisionality. In the adiabatic phase of the pellet ablation and mass relocation when $nT = \text{const}$, the increase of collisionality strongly depends on the pedestal density and temperature changes: $v_{\text{p,pel}}^* = v_{\text{p,0}}^* (T_{\text{p,0}}/T_{\text{p,pel}})^3$, where indexes (0) and (pel) correspond to the values before and after pellet injection. This implies another dependence from the v_p^* -dependent scalings:

$$\Delta W_{\text{ELM},1,2,3} = W_p L_{1,2,3}(v_{\text{p,pel}}^*). \quad (4)$$

It is not discussed in [7] whether or not the reduction of ΔW_{ELM} is connected with changes of the pedestal collisionality. It may appear that pellets of arbitrary sizes could provide desirable mitigation of energy loss if the injection frequency is chosen properly (see Eq. (3)). Thus, in Section 2 we derive the restrictions for the HFS pellet fuelling parameters taking account of Eqs. (1), (3). In Section 3 we analyse ITER scenarios with pellet fuelling taking account of derived restrictions by 1.5D transport simulations. Finally we check the compatibility of ΔW_{ELM} with Eq. (4), based on collisionality.

2. Requirements for Pellet Fuelling System

Let us consider $P_{\text{ELM,lim}}$ from Eq. (1) as the maximum permitted ELM energy density. Then, for the effective ELM energy deposition area, S_{pl} , the ELM energy should be limited by:

$$\Delta W_{\text{ELM}} < S_{\text{pl}} P_{\text{ELM,lim}}, \quad (5)$$

which corresponds to $\Delta W_{\text{ELM}} < 7 \text{ MJ}$ for the effective area of the ELM power deposition on the divertor target $S_{\text{pl}} \sim 6 \text{ m}^2$. This condition gives an estimate for the minimum required pellet injection frequency:

$$f > 0.2 P_{\text{loss}} W_{\text{tot}}/W_{\text{th}} S_{\text{pl}} P_{\text{ELM,lim}}, \quad (6)$$

which corresponds to $f > 3 \text{ Hz}$ for $P_{\text{loss}} \approx 100 \text{ MW}$. Pellet size, d , could be estimated from the particle balance equation. For the ideal case of negligible gas puffing, $Fd^3 N_a f = \langle n \rangle V/\tau_p$:

$$d < (5 S_{\text{pl}} P_{\text{ELM,lim}} \langle n \rangle V \tau_E / \tau_p F N_a W_{\text{tot}})^{1/3}. \quad (7)$$

where τ_p is a particle confinement time, $\langle n \rangle$ is a volume averaged electron density, V is a plasma volume, $N_a = 6 \times 10^{28} \text{ m}^{-3}$ atomic solid hydrogen density in pellet, F is a form factor ($F = 1$ for cubic, $\pi/4$ for cylindrical, and $\pi/6$ for spherical pellets). For the reference ITER parameters: $\langle n \rangle = 10^{20} \text{ m}^{-3}$, $V = 830 \text{ m}^3$, $W_{\text{tot}} \approx 350 \text{ MJ}$, and cylindrical pellet Eq. (7) gives $d < 4.6(\tau_E/\tau_p)^{1/3} \text{ mm}$. There are also a few other mutually connected technical and physical restrictions to be taken into account in our analysis. To keep divertor loads at an acceptable level between ELMs we consider fusion power $P_{\text{fus}} < 500 \text{ MW}$. It is expected that plasma profile peaking can noticeably increase the fusion gain $Q = P_{\text{fus}}/P_{\text{aux}}$. It would require the reduction of the auxiliary heating P_{aux} . Taking account of the requirements to keep good confinement with the density below the Greenwald density, n_G , and power loss across the edge transport barrier $P_{\text{loss}} = P_{\text{aux}}(1 + 0.2 Q) - P_{\text{rad}}$ above the L-H threshold, we have:

$$P_{\text{aux}} < 500/Q \text{ MW}, \quad n/n_G < 1, \quad P_{\text{loss}}/P_{\text{L-H}} > 1, \quad (8)$$

where n is a chord averaged density in 10^{20} m^{-3} , $n_G = I_p/\pi a^2$ [9], I_p is plasma current in MA, a is the plasma minor radius in m, $P_{\text{L-H}} = 2.84 B^{0.82} n^{0.58} \text{ Ra}^{0.81} M_i^{-1}$ is a L-H power limit in MW [10], P_{aux} and P_{rad} are respectively the auxiliary input power and core radiation in MW, B is the

toroidal magnetic field in T. Eqs. (5) - (8) establish the boundary of the operational space for pellet fuelled scenarios with moderate ELM loads.

3. Transport Modelling

For pellet injection modelling we use the integrated ablation/mass relocation model SMART which demonstrated satisfactory agreement with analysed DIII-D and ASDEX-U experiments [11]. For pellet model benchmarking in the extreme case of pellet ablation localised at the very edge we use JT-60U experiments with HFS edge-localised absorption [12] similar to ITER. In this benchmarking the target plasma and pellet injection parameters were chosen correspondent to JT-60U ELMy H-mode experiments with the HFS pellet injection. Four discharges were analysed with the NB heating power in the range 9-22 MW. In these experiments propagation of cool layer induced by pellet is determined from fast electron cyclotron emission (ECE) measurements. The comparison reveals good agreement between modelling predictions and experimental data. Typical results are shown in Fig.1. The pellet ablation proceeds at the very edge. Temperature cooling due to mass relocation is noticeably deeper in agreement with the measurements.

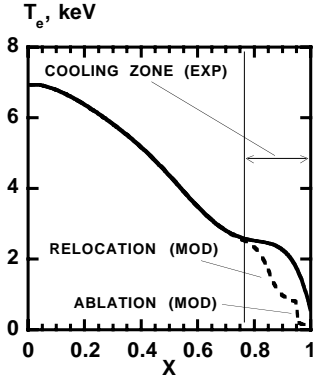


FIG.1. Comparison of HFS pellet induced cooling zones calculated with SMART model [11] and determined from the JT-60U experimental measurements. Solid curve corresponds to measured target plasma T_e profile before pellet injection. Dashed curve corresponds to the model predictions of T_e changed by pellet.

The pedestal energy W_p and local values $T_{p,0}$, $n_{p,0}$ depend on the transport model and fuelling parameters and require transport calculations to estimate $\Delta W_{\text{ELM}}(v_{p,\text{pel}}^*)$ from the v_p^* -dependent scalings. For predictive 1.5D transport simulations of ITER scenarios, we use the ASTRA code [13] with a predictive model [11] for pellet ablation and mass relocation. For the simulations of ITER performance, thermal, toroidal momentum and particle diffusivities χ_e , χ_i , χ_ϕ , D_{He} , D_e of similar form are chosen:

$$D = C_1 f(x) h(x) + C_2 (1 - h(x)) \chi^{\text{neo}}, \quad (9)$$

where $h(x) = 1$ for $x < x_{0.95}$ and $h(x) = 0$ for $x > x_{0.95}$ (corresponding to the H-mode edge pedestal transport improvement to neoclassical value), $x = r/r_a$ is the normalised radius, connected with the toroidal magnetic flux Φ ($r = (\Phi/\pi B)^{1/2}$ and B is the toroidal magnetic field), $x_{0.95}$ is a position of the surface correspondent to the 95% of poloidal flux. For ITER scenarios this simplified description of the edge pedestal gives a pedestal pressure gradient within the ballooning limit which is consistent with the type-I ELM regime considered. The relation between normalisation constants and radial profile correspond to [14]: $\chi_i/\chi_e = 2$, $\chi_i/\chi_\phi = D_e/\chi_e = D_{\text{He}}/D_e = 1$, $f(x) = 1 + 3x^2$. The energy deposition is peaked at the centre. Particle source from pellet fuelling is localised at the edge region with higher diffusivity. Thus, assumed radial dependence $f(x)$ enables estimates of $\tau_E/\tau_p \sim 3-4$ and $d < 7$ mm to be made for the ITER reference scenario. The normalisation factor C_1 is fitted to provide the prescribed behaviour of the energy confinement time τ_E according to experimental scaling, i.e. $H_{98(y,2)} = 1$ [15]. Constant $C_2 = \chi_p/\chi^{\text{neo}}$ is varied to test sensitivity to the pedestal transport coefficient χ_p . The atomic influx of the recycled He is prescribed to be equal to the fusion helium source. Edge fuelling by gas puffing is kept below 10^{22}s^{-1} . The results of 1.5D transport simulations of the ITER plasma with transport coefficients Eq. (9) and pellet fuelling are presented in Table I and Fig. 2. Plasma parameters correspond to the reference scenario: $R/a = 6.2/2$ m, $I_p = 15$ MA, $B = 5.3$ T. Input power is reduced to 24 MW (17 MW of the off-axis NB injection and 7 MW of the central RF heating). DT pellet fuelling is considered with frequency $f = 4$ Hz and pellet speed $v_p = 500$ m/s from the HFS inclined injector. For the considered ITER operational

scenario (see Table. I) the pedestal energy content could be estimated as $W_{p,0} \approx 0.048 n_{p,0} T_{p,0} V \approx 130$ MJ. This value coincides within the error-bars with 150 MJ predicted for ITER by the empirical scaling [16] and lies between the estimates of 80-170 MJ, predicted in [17].

TABLE I: OPERATIONAL RANGE AND PELLETT SIZE SENSITIVITY TO PEDESTAL TRANSPORT.

χ_p/χ^{neo}	$n_{p,0}(10^{20} m^{-3})$	$T_{p,0}(keV)$	d (mm)	n/n_G	P_{loss}/P_{L-H}	$P_{fus}(MW)$	Q
1	0.65	5	6.6	0.86-0.945	1.59-1.26	466	19.4
0.5	0.8	4	5.7	0.85-0.904	1.57-1.36	463	19.3
0.25	0.9	3.6	4.7	0.82-0.85	1.57-1.46	452	18.9

The ELM mitigation compatible with high Q-operation assumes that the spontaneous ELM frequency is smaller than pellet injection frequency, that each pellet triggers one ELM and the pedestal temperature recovery time is shorter than the period of pellet-induced ELMs. We have checked such compatibility for the reference case $\chi_p/\chi^{neo} = 1$. The spontaneous ELM amplitude is calculated from collisionality-based scalings $\Delta W_{ELM,0} = W_{p,0} L_{1,2,3}(n_{p,0}, T_{p,0})$. Then we have from Eq. (3) the estimate for spontaneous ELM frequency $f_0 = 0.2 W_{tot}/\tau_E \Delta W_{ELM,0} \approx 1.4 - 0.54$ Hz which is lower than $f = 4$ Hz as is required. In our simulations temperature recovery time appeared to be shorter than the pellet injection period. Further studies with physics based transport models are required to take into account possible influence of profile stiffness on pellet fuelled scenarios.

Let us also check what will be energy loss reduction in the pellet induced ELM assuming that this loss depends on the pedestal collisionality v_p^* as it was reported from many tokamaks (Fig. 3). Reduction of $\Delta W_{ELM}/W_p$ is based on the assumption that an ELM is triggered at some moment during the pellet injection when the pedestal density (temperature) increases (decreases) and consequently $\tau_{||}$ or v_p^* increases similarly to that found by experiment. In our simulation, at the pedestal position the temperature drops to $T_{p,peel} \sim 1$ keV. Assuming that the ELM is generated at the adiabatic phase of the pellet ablation we evaluate ΔW_{ELM} from v_p^* -based scalings: $\Delta W_{ELM,1} \approx 3.5$ MJ, $\Delta W_{ELM,2} \approx 4.2$ MJ, $\Delta W_{ELM,3} \approx 6.9$ MJ. These estimates can meet the ELM power loss requirement (1). They are also close to the $\Delta W_{ELM,4} \approx 4.6$ MJ predicted by scaling Eq. (3) for pellet frequency $f = 4$ Hz. From these estimates both approaches look compatible for the considered scenario.

For pedestal area $x > x_{95}$ the temperature drops to $T_{peel} \sim 0.8$ keV, but the pedestal top point itself with $T_{peel} \sim 1$ keV is located at the zone with very steep temperature gradient (240 eV/cm). Thus, for strong dependence $v_{p,peel}^* = v_{p,0}^* (T_{p,0}/T_{p,peel})^3$ our estimate for $\Delta W_{ELM,peel}$ is beyond the accuracy of the model assumptions. But in the presence of strong temperature gradients it is difficult to expect that the temperature value at any single point is critical to the entire process. Therefore, some sort of averaged parameters could be more adequate to the description of the process. It follows from our calculations that the reduced pedestal diffusivity χ_p requires a reduction in the size of the pellet. The pedestal density becomes higher and the temperature drops (Table I), therefore, the pedestal collisionality increases as well. But the effect of pellets on the pedestal collisionality also becomes smaller. Thus, if the increase of the collisionality is a key point for ELM mitigation, then attenuation of the entire scenario with the pedestal transport will be required. In the case when the pedestal collisionality does not play such a critical role for ELM energy loss in ITER similar to JT-60U [4], the analysis of such details is not required.

It would also be necessary to analyse possible plasma confinement deterioration caused by pellet injection. It could be, in particular, connected with NTM seeding island appearance caused by pellet mass relocation to $q = 2$ magnetic surface and profile stiffness. To estimate the flexibility of the fuelling parameters, further experimental analysis is required. It is necessary to identify the physical basis of collisionality-dependent and frequency-dependent experimental scalings.

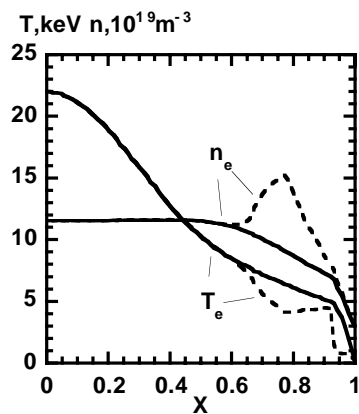


FIG.2. Electron density $n(x)$ and temperature $T(x)$ profiles at the moments before (solid line) and after (dashed line) pellet injection.

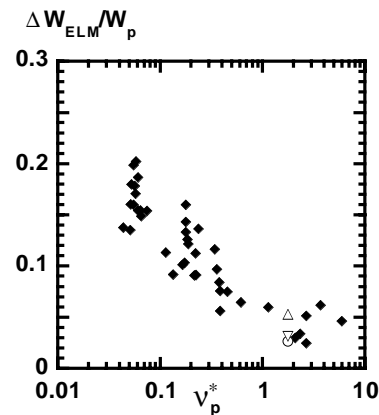


FIG.3. Dependence of fraction of pedestal energy loss $\Delta W_{ELM}/W_p$ in ELMs on the pedestal collisionality v_p^* . Experimental points [5] are shown by diamonds together with scaling predictions $L_1(\circ)$, $L_2(\nabla)$, $L_3(\Delta)$ for ITER with pellet fuelling.

4. Conclusions

In summary, this investigation has shown that the ELM loss mitigation derived from the experimental scalings implies restrictions on the pellet injection. Calculations reveal that the HFS injection of a pellet with moderate size ($d < 0.7$ cm) and speed ($v_p = 0.5$ km/s) would enable reduction of the fractional ELM energy loss to less than 5%, while keeping the plasma in the H-mode, the density below the Greenwald density, $P_{fus} < 500$ MW, $P_{loss} < 100$ MW and the confinement enhancement factor corresponding to the type-I ELMy H-mode scaling $HH_{98y,2} \sim 1$, with high $Q \sim 20$. The estimated pellet induced ELM energy loss in the considered scenario is compatible with collisionality-dependent and frequency-dependent experimental scalings.

References

- [1] FEDERICI, G., et al., "Key ITER Plasma Edge and Plasma-Material Interaction Issues", 15th International Conference on Plasma Surface Interactions in Controlled Fusion devices, Gifu, Japan, 27 May-1 June, 2002.
- [2] JANESCHITZ, G., et. al., J. Nucl. Materials 290-293 (2001) 1.
- [3] LOARTE, A., et al, "Multimachine Comparison of Type I ELM Energy and Particle Losses and Implications for ITER", ITPA Pedestal and Divertor Physics Meeting, Feb 2002, San Diego.
- [4] OYAMA, N., et.al, Submitted to Nuclear Fusion.
- [5] LOARTE, A., et al, IAEA-CN-77/ITER/2-ITERP/11, 18 IAEA Fusion Energy Conference, (2000).
- [6] SAIBENE, G., JONES, T.T.C., "H-mode Density Limit and Confinement with Pellet and Gas Fuelling", in JET report JET-R(00)02, "Descriptive Analysis of 1999 Task Force Data", (2000).
- [7] LANG, P., et al., 29th EPS Conf. on Plasma Phys. and Contr. Fusion, ECA, Vol. **26B**, P-1.044 (2002).
- [8] HERRMANN, A., "Overview on stationary and transient divertor heat loads", PPCF **44** (2002) 883.
- [9] GREENWALD, M., PPCF **44** (2002) R27.
- [10] SNIPES, J.A., PPCF **42** (2000) A299.
- [11] POLEVOI, A.R., SHIMADA, M., PPCF, **43** (2001) 1525.
- [12] TAKENAGA, H., and the JT-60 Team, Phys. of Plasmas **8**, (2001) 2217.
- [13] PEREVERZEV, G., et. al. Report IPP 5/42 (1991).
- [14] POLEVOI, A., et al., "ITER Confinement and Stability Modelling", J. Plasma Fusion Research, SERIES Vol.5 (2002), to be published.
- [15] KARDAUN, O, et al., 18th IAEA Fusion Energy Conference, Sorrento, Italy (2000) ITERP/04.
- [16] SUGIHARA, M., et al., "Examinations on pedestal pressure based on database v3", 2nd ITPA Meeting on H-mode Edge Pedestal Physics, 26-28 Feb. 2002, San Diego, USA.
- [17] CORDEY, J.G., et al., IAEA-CN-94/CT/P-02, this Conference.